

ORIGIN OF ARISTARCHUS OLIVINE BASED ON M3 AND DIVINER ANALYSES. S. M. Wiseman¹, K. L. Donaldson Hanna¹, J. F. Mustard¹, P. J. Isaacson², C. M. Pieters¹, B. Jolliff³, ¹Brown University (sandra_wiseman@brown.edu), ²University of Hawaii at Manoa, ³Washington University in St. Louis.

Introduction: The Copernican-aged Aristarchus impact crater occurs on the SE margin of the Aristarchus plateau, which is located to the west of the Imbrium basin (Fig 1). The plateau was likely uplifted as a consequence of the Imbrium event [e.g., 1,2,3]. Aristarchus crater occurs near the contact between plateau materials and western Oceanus Procellarum basalts, which embay the plateau (Fig 1). The impact event postdates Vallis Shroteri and impact implaced materials overlie pyroclastic deposits [e.g., 4] on the plateau. Materials with variable compositions are exposed in an around the crater [e.g., 4,5,6]. Of particular interest is the origin of olivine-bearing deposits that occur as ejecta overlying the SE portion of the crater rim [7].

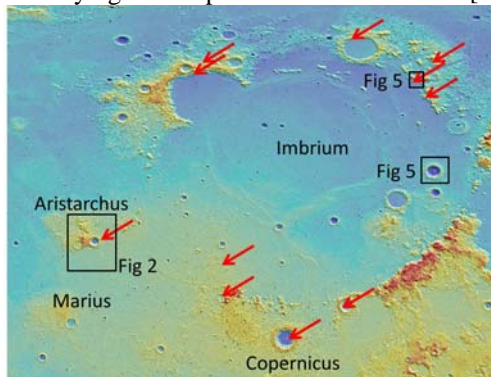


Figure 1. WAC color coded topography overlain on shaded relief. Red arrows indicate olivine exposures [8].

M³ and Diviner Data: The Chandrayaan-1 Moon Mineralogy Mapper (M³) is a visible to near infrared (0.43-3.0 μ m) imaging spectrometer [9]. We used data acquired at a global mapping resolution of 140 m/pixel with 85 channels. M³ data were radiometrically calibrated and photometrically corrected (PDS level 2).

The Lunar Reconnaissance Orbiter Diviner Lunar Radiometer Experiment acquires data from 0.3 to 200 μ m in 9 channels [10]. Channels centered at 7.8, 8.2, and 8.6 μ m allow estimation of the Christiansen Feature (CF), an emissivity maximum at mid-infrared wavelengths that is diagnostic of composition [11].

Aristarchus Crater: Some material exposed by the Aristarchus impact has a high albedo (Fig 2). These bright exposures have been interpreted to contain anorthosite [4,5]. Investigations by [12] found crystalline plagioclase features in the central peak, though this feature near 1.25 μ m is not readily apparent at the spatial resolution of M³. Bright material in SW ejecta was inferred to be silicic due to short CF positions identified in Diviner data [13].

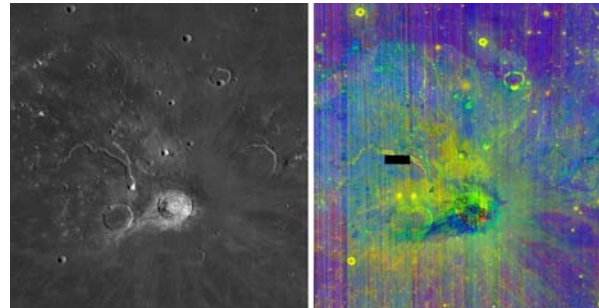


Figure 2. (left) Subset of WAC global mosaic showing Aristarchus crater. (right) M³ spectral parameter color composite with R=1.05 μ m band depth, G=integrated band depth at 2 μ m, and B=0.95/0.75 μ m. Red indicates olivine.

NW portions of the rim and ejecta expose plateau materials and are spectrally dominated by pyroxene in the VNIR and exhibit both 1 and 2 μ m absorptions (Fig 3). The olivine-bearing material exposed in the SE ejecta (Fig 3, red arrow) is spectrally dominated by olivine, although a subtle absorption at 2 μ m could be caused by pyroxene and/or spinel [7] (Fig 3).

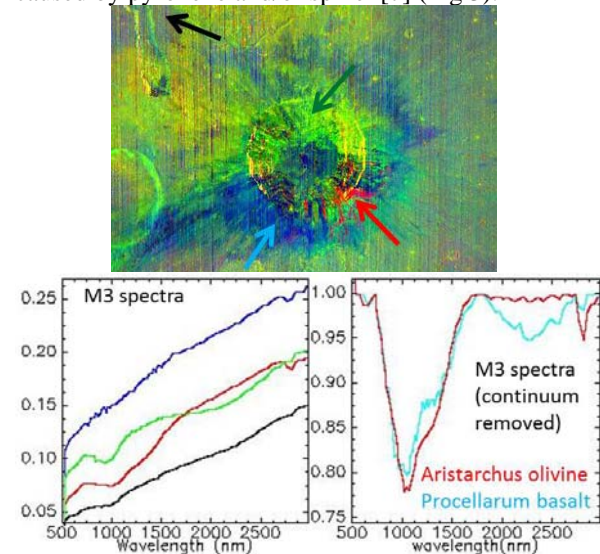
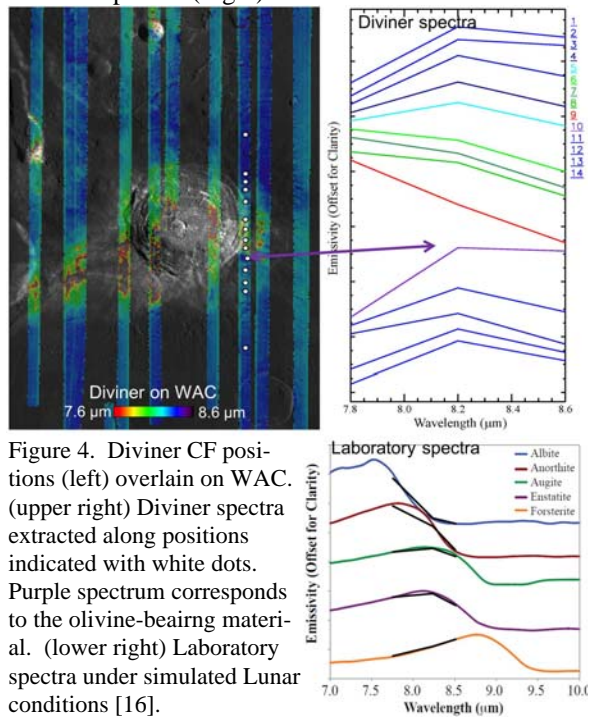


Figure 3. (upper) Zoom in of Aristarchus crater (Fig 2). (left) Spectra extracted from locations with arrows. (right) continuum removed spectra, cyan spectrum extracted from olivine-bearing Procellarum basalt – purple unit in Fig 2).

Although the olivine-bearing material is dissimilar from other materials exposed in the crater, olivine-bearing western Procellarum basalts [e.g.,14] are exposed to the north of the plateau and olivine-bearing flows originating from the Marius Hills [e.g., 15] occur to the south. However, the western Procellarum and Marius Hills units exhibit distinct pyroxene related

absorptions in addition to olivine features (Fig 3, lower right). The olivine-bearing material exposed in the SE Aristarchus ejecta is spectrally distinct from olivine-bearing western Procellarum and Marius Hills basalts.

Although VNIR spectra of the olivine-bearing ejecta deposits are dominated by olivine, it is important to note that Fe-poor phases that may be mixed with the olivine are spectrally neutral and difficult to detect in the VNIR. Based on the geologic context, it is likely that the olivine-bearing ejecta is mixed with spectrally neutral material similar to the blue exposures in Fig 3. Diviner spectra are consistent with a mixture of olivine and other phases (Fig 4).



Origin of Olivine: Potential sources of the olivine-bearing material excavated by the impact include western Procellarum or Marius Hills basalts. Both the Procellarum basalts [e.g., 14] and some units associated with the Marius Hills [15] are olivine-bearing. However, these materials also have significant pyroxene spectral contributions which are not observed in the Aristarchus ejecta. As the olivine is associated with impact melt and ejecta, impact processes may have played a role.

Alternatively, the olivine-bearing deposits could be derived from a shallow pluton that is not represented by other surface exposures (perhaps related to the formation of the plateau and/or pyroclastic deposits) or re-excavated material originally deposited by the Imbrium forming event. Several olivine-bearing deposits have been detected in the vicinity of Imbrium [8]. Such deposits may have been excavated from the low-

er crust/ upper mantle [17]. There are several olivine bearing deposits in the vicinity of Imbrium [8]. We investigated these deposits and looked for additional deposits using M^3 data. Some of these deposits (e.g., Fig 5) are spectrally dominated by olivine, although the spectra are not as spectrally pure as the Aristarchus olivine-bearing spectra. This may be because the deposits are smaller and thus more likely to be spatially mixed with other material. One such deposit is exposed in a crater and another deposit occurs in blocky material that is likely Imbrium ejecta (Fig 5).

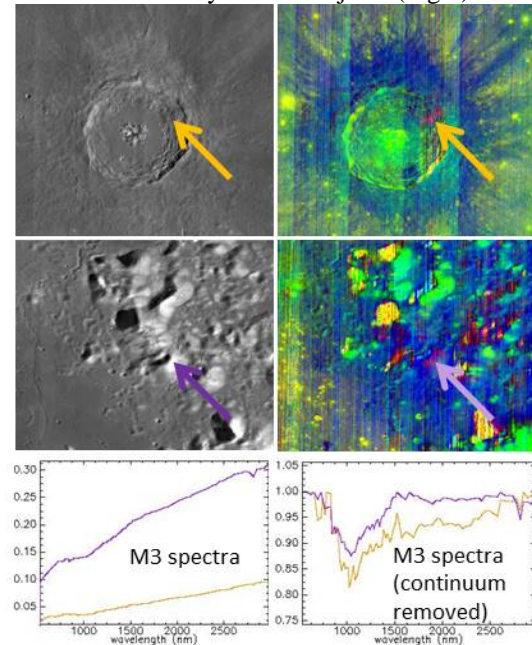


Figure 5. M^3 image subsets, locations shown in Fig 1. Parameters same as in Fig 2. Red indicates olivine.

Discussion and Future Work: Given that spectrally similar deposits to those of the olivine-bearing Aristarchus ejecta are found in other exposures in the vicinity of Imbrium, the deposit in Aristarchus may represent re-exposed Imbrium ejecta. Future work will focus on spectral modeling of M^3 and Diviner spectra to determine the abundance and Mg# of the olivine exposed in Aristarchus and the vicinity of Imbrium.

References: [1] H. J. Moore (1965) *U.S. Geol. Survey, Geol. Invest. Map*, I-465, [2] J. E. Guest (1973) *Geol. Soc. Am. Bull.*, 84, [3] S. H. Zisk et al (1977) *Moon*, 17, [4] McEwen et al (1994) *Science*, 266, [5] Lucey et al (1986) *JGR*, 91, [6] Le Mouelic et al (1999) *GRL*, 26, [7] Mustard et al (2011) *JGR*, 116, [8] Yamamoto et al (2010) *Nat. Geosci.*, 3, [9] Pieters et al., (2011) *JGR* 116, [10] D. A. Paige et al. (2009) *Space Sci. Rev.*, 150, [11] J. E. Conel (1969) *JGR* 74, [12] Ohtake et al (2009) *Nature*, 461, [13] Glotch et al (2010) *Science*, 329, [14] Staid et al (2011), *JGR*, 116, [15] Besse et al (2011) *JGR*, 116, [16] Donaldson Hanna et al (2011), *JGR*, in press, [17] Stewart (2011) *LPSC* 42, 1633.